Biomimetic Copper–O_2 Chemistry

DOI: 10.1002/anie.201409709

A Ferromagnetically Coupled ($S = 1$) Peroxodicopper(II) Complex**

*Nicole Kindermann, Eckhard Bill, Sebastian Dechert, Serhiy Demeshko, Edward J. Reijerse, and Franc Meyer**

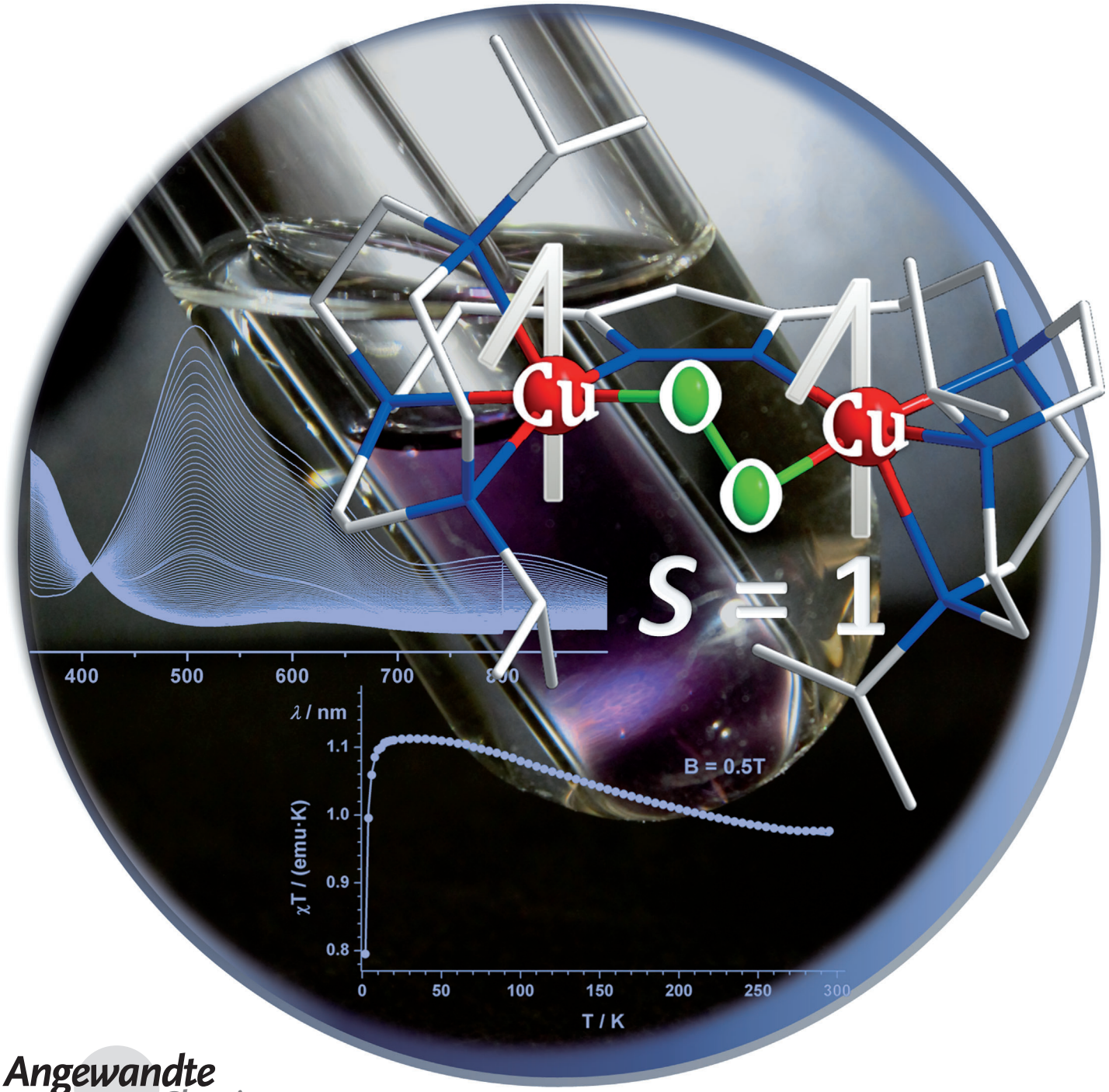

Abstract: *Copper enzymes play important roles in the binding and activation of dioxygen in biological systems. Key copper/dioxygen intermediates have been identified and studied in synthetic analogues of the metalloprotein active sites, including the μ-η²:η²-peroxodicopper(II) motif relevant to type III dicopper proteins. Herein, we report the synthesis and characterization of a bioinspired dicopper system that forms a stable μ-η¹:η¹-peroxo complex whose Cu-O-O-Cu torsion is constrained to around 90° by ligand design. This results in sizeable ferromagnetic coupling between the copper(II) ions, which is detected by magnetic measurements and HF-EPR spectroscopy. The new dicopper peroxo system is the first with a triplet ground state, and it represents a snapshot of the initial stages of O_2 binding at type III dicopper sites.*

Investigations on binding and activation of dioxygen at dinuclear copper sites have been motivated by the fascinating chemistry exhibited by metalloproteins containing a dicopper active site. These comprise the type III copper proteins hemocyanin, catechol oxidase, and tyrosinase[1] as well as particulate methane monooxygenase.[2] The development of synthetic analogues had tremendous impact on the understanding of those biological systems[3–6] and gave rise to the isolation and characterization of different types of intermediates that occur in the reaction of copper(I) complexes with dioxygen, namely with a *trans*-μ-η¹:η¹- (**^{T}P**, see Scheme 1), μ-η²:η²-peroxodicopper(II) (**^{S}P**), or bis(μ-oxo)dicopper(III) (**O**) core.[7–10] In type III copper proteins, the butterfly-shaped **^{S}P** motif is the common detectable intermediate upon O_2 binding and activation, though it cannot be excluded that the bis(μ-oxo)dicopper(III) core **O** is involved in subsequent chemistry.[1,3] In contrast, a **^{T}P** core, which was found in several synthetic systems,[7,11,12] is not considered as biologically relevant. Using the compartmental pyrazolate-based ligand scaffold $[L^{me}]^-$ (Scheme 1) we recently added a missing piece to this bouquet of Cu_2/O_2 motifs, namely the adduct $[L^{me}Cu_2(O_2)]^+$ featuring a *cis*-μ-η¹:η¹-peroxodicopper(II) (**^{C}P**)[13] core whose structural characterization was lacking until then. In addition to some unprecedented side-on interaction of the peroxo unit in $[L^{me}Cu_2(O_2)]^+$ with Lewis acids such as Na^+, the copper(II) ions in $[L^{me}Cu_2(O_2)]^+$ were found to exhibit only weak antiferromagnetic coupling ($-J = 72\ cm^{-1}$),[13] in contrast to all other known peroxodicopper(II) complexes which usually show an $S = 0$ ground state with very large singlet-triplet splitting ($-J \geq 600\ cm^{-1}$). Based on computational work, a **^{C}P** species has indeed been proposed to occur on the trajectory of O_2 activation at type III centers.[14] During initial stages of O_2 binding, upon simultaneous electron transfer from the copper(I) ions to the two orthogonal $\pi^*(O_2)$ orbitals and delocalization of the spin onto the copper ions, the system is still on the triplet surface and ferromagnetic coupling is predicted to prevail in a transient Cu-O-O-Cu arrangement with a close to 90° torsion angle. The Cu_2O_2 core then progresses to the **^{S}P** structure with concomitant evolvement of superexchange coupling that finally favors the singlet state.[14] The weak antiferromagnetic coupling observed for $[L^{me}Cu_2(O_2)]^+$ can thus be rationalized on the basis of its 65.2° torsion angle, which attenuates superexchange but still differs from an orthogonal situation. We reasoned that further elaboration of the pyrazole-based ligand scaffold to allow for shorter Cu···Cu separations should increase the Cu-O-O-Cu torsion angle and should make a ferromagnetically coupled peroxo-dicopper system with triplet ($S = 1$) ground state accessible.

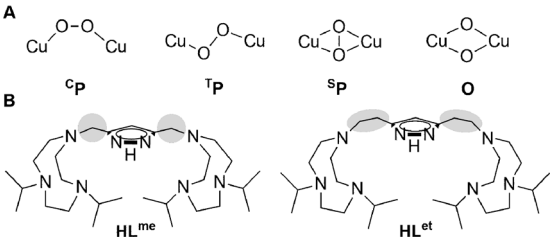

Scheme 1. Dinuclear Cu_2/O_2 motifs that have been found in nature and in synthetic systems (A). Ligand HL^{me} employed in previous work,[13] and the new ligand system HL^{et} used in this work (B). Modifications of the ligand backbone are highlighted in gray.

We had previously shown that the metal···metal distances in pyrazole-bridged bimetallic complexes can be tuned by varying the length of the peripheral spacers within the chelate arms attached to the 3- and 5-positions of the heterocycle.[15] To avoid forfeiting the beneficial stabilizing effect of the side arm triazacyclononane (tacn) units, we chose to follow a different strategy in the present work, namely elongation of the linkages between the central pyrazole and the tacn rings from methylene spacers in HL^{me} to ethylene spacers in HL^{et} (Scheme 1).[16] The multistep synthesis of the new ligand HL^{et}, starting from recently reported pyrazole building blocks,[17,18] is described in the Supporting Information.

Deprotonation of HL^{et} with potassium *tert*-butoxide followed by the addition of two equivalents of $[Cu(MeCN)_4]ClO_4$ and subsequent anion exchange using sodium tetraphenylborate gave the dicopper(I) complex $[L^{et}Cu_2]BPh_4$ (**1**). Crystalline material could be obtained from propionitrile/diethyl ether solutions of **1**, and the molecular structure of **1** has been determined by X-ray diffraction (Figure 1). The copper(I) ions are found in

[*] N. Kindermann, Dr. S. Dechert, Dr. S. Demeshko, Prof. Dr. F. Meyer
Institut für Anorganische Chemie
Georg-August-Universität Göttingen
Tammannstrasse 4, 37077 Göttingen (Germany)
E-mail: franc.meyer@chemie.uni-goettingen.de
Homepage: http://www.meyer.chemie.uni-goettingen.de
Dr. E. Bill, Dr. E. J. Reijerse
Max-Planck-Institut für chemische Energiekonversion
Stiftstrasse 34–36, 45470 Mülheim an der Ruhr (Germany)

[**] Financial support from the Fonds der Chemischen Industrie, the Studienstiftung des deutschen Volkes (to N.K.), and the DFG (International Research Training Group IRTG 1422 "Metal Sites in Biomolecules: Structures, Regulation and Mechanisms"; see http://www.biometals.eu) is gratefully acknowledged. This work was performed in the framework of the COST actions CM 1003 ("Biological oxidation reactions—mechanisms and design of new catalysts") and CM 1305 (ECOSTBio). We thank Gudrun Klihm, MPI-CEC, for technical assistance and running the HF-EPR measurements.

Supporting information for this article is available on the WWW under http://dx.doi.org/10.1002/anie.201409709.

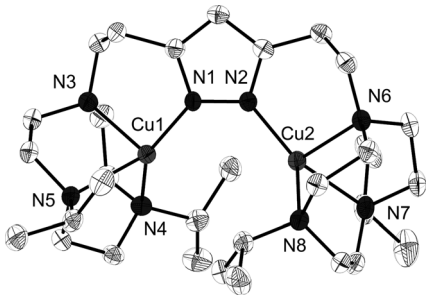

Figure 1. Molecular structure of the cation of **1**, thermal ellipsoids set at 50% probability. BPh_4^- ion and hydrogen atoms have been omitted for clarity.

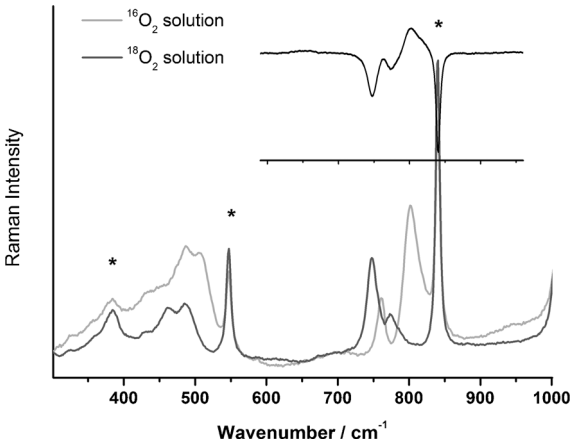

Figure 2. Resonance Raman spectrum of **2** in propionitrile at room temperature ($\lambda_{ex} = 633$ nm); the $^{16}O_2$ spectrum is in light gray and the $^{18}O_2$ spectrum in gray. The inset (black line) shows the difference spectrum in the O–O stretch region. Residual solvent signals are marked with an asterisk (*).

trigonal-pyramidal coordination environment composed of three N-atoms of a tacn unit and one pyrazole-N. The pyrazolate bridge spans the two metal ions with a Cu···Cu distance of 3.968 Å, which is indeed shorter than in $[L^{me}Cu_2]^+$ (4.153 Å).[19] Air-sensitive **1** has been fully characterized by ^1H and ^{13}C NMR as well as IR spectroscopy, ESI mass spectrometry (ESI-MS) and elemental analysis (see Supporting Information).

Treatment of **1** in acetone or propionitrile with air or dry dioxygen at room temperature immediately led to intensely purple-colored solutions, indicating the formation of a dioxygen adduct $[L^{et}Cu_2(O_2)]BPh_4$ (**2**). Monitoring the reaction by UV/Vis spectroscopy showed the growth of a principal new band at 506 nm ($\varepsilon \approx 4800\,M^{-1}cm^{-1}$) and a shoulder around 600 nm ($\varepsilon \approx 2800\,M^{-1}cm^{-1}$). These absorptions, assigned to peroxide→Cu^{II} charge transfer (CT) transitions, are typical for μ-η^1:η^1-peroxodicopper(II) species ^{T}**P** and ^{C}**P**.[10,13] A resonance Raman (rR) spectrum of the dioxygen adduct $[L^{et}Cu_2(O_2)]^+$ ($\lambda_{ex} = 633$ nm) exhibits two features that are sensitive to oxygen isotopic labeling, namely at 803 cm^{-1} ($\Delta^{16}O_2-^{18}O_2 = 54\,cm^{-1}$) and at 512 cm^{-1} ($\Delta^{16}O_2-^{18}O_2 = 22\,cm^{-1}$). For natural abundance dioxygen (light gray spectrum, Figure 2), besides the peak at 803 cm^{-1} that reflects the peroxide O–O stretch, there is a band at around 760 cm^{-1}, which is probably due to Fermi resonance; this phenomenon has also been observed in the ^{C}**P** model $[L^{me}Cu_2(O_2)]^+$ and in several reported ^{T}**P** species.[13,20,21] The peak at 512 cm^{-1} is assigned to the Cu–O stretch; it is poorly resolved in the solution spectrum but very distinct in the solid state spectrum (see Supporting Information for details). Both the $\nu_{O\text{-}O}$ and $\nu_{Cu\text{-}O}$ frequencies are slightly higher than found for the ^{C}**P** model $[L^{me}Cu_2(O_2)]^+$,[13] but significantly lower than usually observed for ^{T}**P** complexes.[10] For the ^{C}**P** model $[L^{me}Cu_2(O_2)]^+$ this has been ascribed to a reduced degree of Cu–O covalency, in accordance with significantly lower extinction coefficients for the peroxide→Cu^{II} CT transitions (mostly greater than $10^4\,M^{-1}cm^{-1}$ in ^{T}**P** complexes).[13] Note that in contrast to other well-studied examples of *cis*/*trans*-μ-η^1:η^1-peroxo complexes, such as stable diamagnetic dicobalt(III) species,[22] UV/Vis spectroscopic signatures of μ-η^1:η^1-peroxodicopper(II) complexes are relatively insensitive to differences in the M-O-O-M torsion angle as found for $[L^{me}Cu_2(O_2)]^+$ or the new $[L^{et}Cu_2(O_2)]^+$, or non-distorted ^{T}**P** systems. Whereas in dicobalt(III) peroxo complexes the CT absorption bands change dramatically upon varying the M-O-O-M dihedral angle because of mixing of the π^*_v and π^*_σ orbitals upon distortion, such mixing is present in all dicopper(II) peroxo complexes because the individual metal ion's coordination environment deviates from an ideal trigonal-bipyramidal or square-pyramidal polyhedron,[23] leading to similar spectroscopic features for both the ^{C}**P** and ^{T}**P** forms.

Single crystals of $[L^{et}Cu_2(O_2)]BPh_4$ (**2**) suitable for X-ray diffraction were grown from an acetone/diethyl ether mixture of **2** at −20 °C. Crystalline material is stable for at least several weeks at room temperature on air without any obvious change. The molecular structure of **2** (Figure 3) indeed confirms the μ-η^1:η^1-peroxodicopper(II) core with d(O–O) = 1.460 Å and a very short Cu···Cu separation of 3.677 Å which is compressed compared to the ^{C}**P** model $[L^{me}Cu_2(O_2)]^+$ (3.797 Å)[13,24] and much shorter than the Cu···Cu distances in all known ^{T}**P** species (over 4.35 Å).[7,11,12] For **2**, φ is the Cu-O-O-Cu torsion angle around the O–O axis as defined in Figure 3 is 104.2°, which differs significantly from the value for the ^{C}**P** model system ($\varphi = 62.5°$).[13] It thus is quite close to the sought-after $\varphi = 90°$ situation and can be viewed as intermediate between the *cis* (^{C}**P**) and *trans* (^{T}**P**) configurations.

The coordination environment of each copper(II) ion in **2** is approximately square-pyramidal ($\tau = 0.20$)[25] with relatively long Cu1–N5 and Cu2–N8 bonds forming the local z-axes. Hence, the local spin densities should be found in the copper $d_{x^2-y^2}$ orbitals that point to the adjacent peroxide-O atoms and form σ-bonds with corresponding oxygen p_x and p_y orbitals, respectively. This electronic structure description is supported by the results of preliminary DFT studies (Figure 4; B3LYP hybrid functional, def2-tzvp and def2-tzvp/j basis sets; see Supporting Information for details). The large Cu-O-O-Cu torsion angle close to 90° should suppress antiferromagnetic superexchange between the copper(II) ions because there is negligible overlap of the magnetic orbitals in the exchange pathway through the O–O bridge

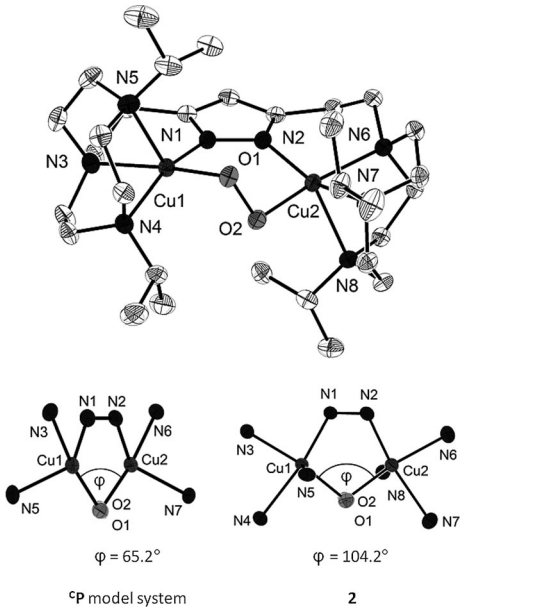

Figure 3. Top: Molecular structure of the cation of **2**, thermal ellipsoids set at 50% probability; the BPh_4^- ion, solvent molecules, and hydrogen atoms have been omitted for clarity. Bottom: Comparison of the core structures of the recently reported **^{c}P** model system $[L^{me}Cu_2(O_2)]^+$ (left)[13] and the new peroxo complex **2** (right) presented herein. Both show the torsion angle φ, looking along the O1–O2 bond (N4 and N8 for **^{c}P** model are omitted for clarity).

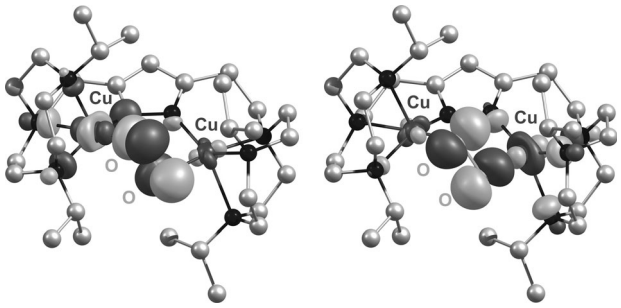

Figure 4. α-HOMO (left, contour value = 0.05) and α-HOMO−1 (right, contour value = 0.05) of the $S=1$ state of **2**.

($S_{overlap} = 0.003$ according to DFT calculations, see Supporting Information). In this situation genuine ferromagnetic exchange can dominate and stabilize the coupled $S=1$ ground state, as it has been predicted, for example, for the initial stages of O_2 binding in hemocyanin.[14] Magnetic susceptibility data of compound **2**, collected with microcrystalline powder samples in the temperature range 2–295 K at 0.5 T, indeed show a distinct maximum of $\chi_m T$ at approximately 30 K (Figure 5A), which indicates sizeable ferromagnetic spin coupling. A first simulation, using an isotropic Heisenberg–Dirac–VanVleck spin Hamiltonian ($H_{HDVV} = -2JS_1 \cdot S_2$), yielded a notably large positive exchange coupling constant, $J = +72\ cm^{-1}$. Hence, the ground state of **2** is a very well-stabilized total-spin triplet, $S=1$.

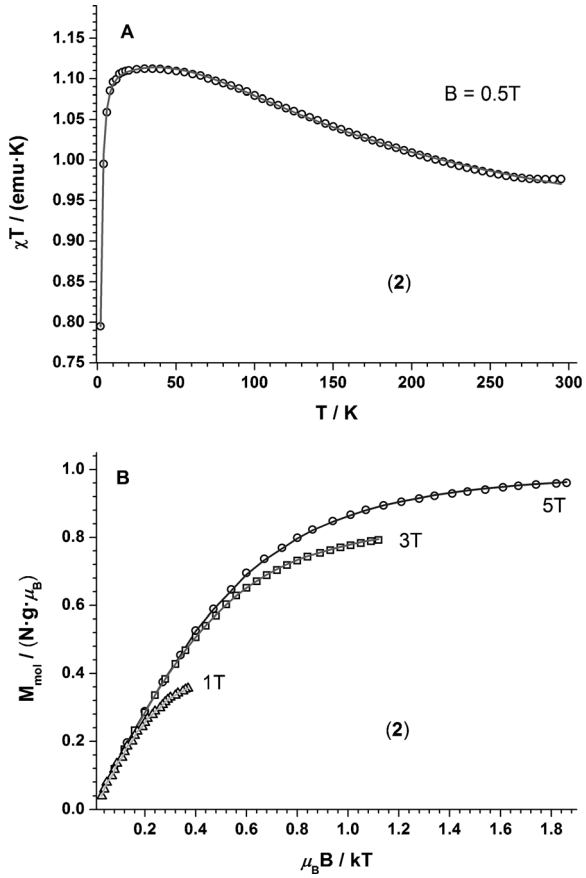

Figure 5. $\chi_m T$ vs. T measurement in the temperature range of 2–295 K at 0.5 T (A) and variable temperature/variable field (VTVH) magnetization measurements at fields of 1 T, 3 T, and 5 T presented as M_{mol} vs. $\mu_B B/kT$ (B) for crystalline samples of **2**. The solid lines represent the best global fit for both data sets, including antisymmetric DM interaction.

Intriguingly, multi-field magnetization data of **2** recorded at 1, 3, and 5 T show considerable nesting of $M(\mu_B B/kT)$ (Figure 5B), which indicates, just like the strong decrease of $\chi_m T$ below 20 K, rather strong zero-field splitting (ZFS) of the order $D \approx 3\ cm^{-1}$ (alternative simulations assuming intermolecular interactions did not give reasonable fits, see Figure S1). Such strong ZFS is unexpected for a spin-pair such as **2**, as the local spin doublets, $S_i = {}^1/_2$, cannot contribute single-ion ZFS, and through-space dipole–dipole coupling is orders of magnitudes weaker because of the long Cu···Cu distance (a point dipole model would yield $D_{dd} = 0.05\ cm^{-1}$ for $r = 3.68$ Å and $g_\perp = 2.06$, according to the relation $D_{dd} \approx 0.65\ g_\perp{}^2/r^3$).[26,27] Thus we conclude that the HDVV Hamiltonian is insufficient to describe **2**. Higher-order exchange terms, such as anisotropic or antisymmetric exchange interactions, must be present, arising from the combined actions of single-ion spin-orbit coupling (SOC) and mutal (super)exchange-coupling between ground and excited states of the paramagnetic ions.

Although antisymmetric exchange (Dzialoshinsky–Moriya interaction, DM)[28,29] is a first-order SOC effect of the magnitude $(\Delta g/g)\,|2J|$, whereas anisotropic exchange is second order, $(\Delta g/g)^2\,|2J|$, it has been rarely observed for

copper(II) dimers because it obeys a number of symmetry rules, and in particular it vanishes for symmetric dimers with inversion symmetry. However, antisymmetric (DM) exchange has been investigated theoretically[30–32] and identified as the leading non-HDVV interaction that may cause sizeable ZFS effects for trimeric molecules with 'spin frustration', since in those cases the pairs of individual copper(II) or other paramagnetic ions are not related by symmetry.[33–35] Following this approach for asymmetric **2** by including antisymmetric exchange in the spin Hamiltonian [Eq. (1)]

$$\hat{H} = -2J\vec{S}_1 \cdot \vec{S}_2 + \vec{d} \cdot \vec{S}_1 \times \vec{S}_2 + \mu_B\left(\vec{S}_1 + \vec{S}_s\right) \cdot g \cdot \vec{B} \qquad (1)$$

where $\vec{d}$ is the DM pseudovector, we obtained excellent global fits for both magnetic data sets shown in Figure 5, including $\vec{d} = (0,\ 0,\ 42)\ \mathrm{cm}^{-1}$ and $g = (2.06,\ 2.06,\ 2.253)$ (whereby for the sake of less ambiguity the g matrices were taken axial and collinear to each other with $\vec{d}$ parallel to z). The large ZFS of the triplet ground state should prevent EPR transitions of **2** at X-band frequencies ($h\nu \approx 0.3\ \mathrm{cm}^{-1}$). Accordingly, the compound was found to be EPR-silent at X-band and Q-band frequencies in the solid state and solutions. To further substantiate the presence of DM interaction for the copper(II) ions in **2** we performed preliminary HF-EPR measurements at 240 GHz and in fact found a number of resonances that strongly resemble the pattern expected for spin triplets with strong ZFS somewhat smaller than $h\nu$ (i.e. $|D| < 8\ \mathrm{cm}^{-1}$). This result excludes dipole-interaction only, but corroborates the interpretation of the magnetization data. Unfortunately, however, the resonance fields of some of the HF-EPR lines appeared to be somewhat temperature dependent, which we presently cannot explain. A preliminary fit to the 10 K spectrum with $|D| = 2.15\ \mathrm{cm}^{-1}$ is shown in Figure S2.

ESI-MS of MeCN solutions of the peroxo complex **2** shows only signals for $[L^{et}Cu_2]^+$, suggesting that binding of O_2 is reversible under ESI-MS conditions. However, the stability of **2** in the solid state and in solution is rather high: depending on the purity of the starting material, it exhibits a half-life of approximately 10 h in propionitrile at room temperature (Figure 6). The thermal decay of **2** finally leads to a light-blue species **3** with absorption maxima at 356 nm ($\varepsilon \approx 3700\ \mathrm{M}^{-1}\mathrm{cm}^{-1}$) and 613 nm ($\varepsilon \approx 200\ \mathrm{M}^{-1}\mathrm{cm}^{-1}$). ESI-MS analysis of solutions of **2** in propionitrile or acetone that were stored at room temperature for several days showed signals solely corresponding to $[L^{et}Cu_2(OH)]^{2+}$ (Figure S6), indicating that a single predominant product is formed. Slow evaporation of acetone solutions of **3** led to the formation of blue single crystals, suitable for X-ray diffraction. This data confirmed the assignment of **3** being a hydroxo-bridged dicopper(II) complex, without any oxygenation of the pyrazole-based ligand (Figure 7). The molecular structure of **3** with $d(\mathrm{Cu}\cdots\mathrm{Cu}) = 3.405$ Å confirms that the new ligand $[L^{et}]^-$ can support shorter metal–metal separations than $[L^{me}]^-$.[13]

In conclusion, we report a first structurally characterized dicopper(II) peroxo complex **2** that has an $S = 1$ ground state and exhibits sizeable ferromagnetic coupling between the two copper(II) ions. This result has been achieved by rational ligand design: the pyrazolate-based binucleating ligand $[L^{et}]^-$ with suitably adjusted length of the chelate arms enforces a Cu···Cu distance much shorter than in all other known μ-η^1:η^1-dicopper-peroxo systems. This gives rise to a Cu-O-O-Cu torsion angle close to 90° and thus to interaction of the two magnetic copper(II) $d_{x^2-y^2}$ orbitals with orthogonal $\pi^*(O_2)$ orbitals, which suppresses the (usually predominant) antiferromagnetic contribution to the magnetic coupling. The unprecedented structural and electronic characteristics of **2**, including some unusually large ZFS of the $S = 1$ state, are reflected in the magnetic and high-field EPR data. Complex **2** can be regarded as a snapshot of the initial stage of O_2 binding in type III dicopper proteins, in accordance with scenarios predicted by computational studies.[14] Further investigations that give more detailed insight into the electronic structure of **2**, and into the reactivity resulting from that electronic structure, are in progress.

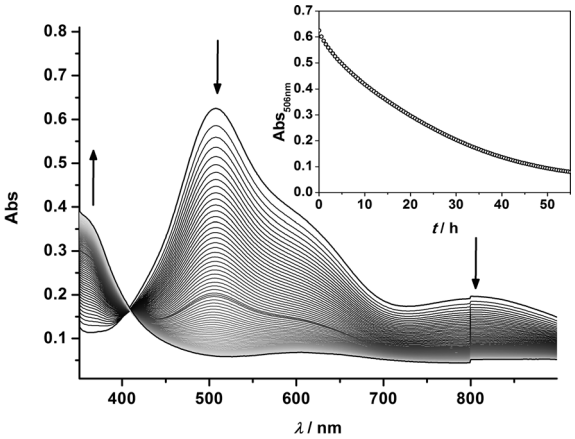

Figure 6. Decay of $[L^{et}Cu_2(O_2)]BPh_4$ (**2**) in propionitrile, monitored by UV/Vis spectroscopy at room temperature, arrows indicating the development of the spectrum over time. The inset shows the time trace of the band at 506 nm.

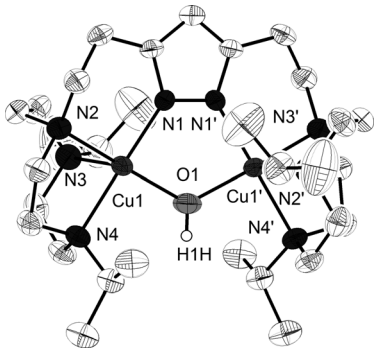

Figure 7. Molecular structure of the cation of **3**, thermal ellipsoids set at 50% probability. BPh_4^- ions, solvent molecules, and all hydrogen atoms except for H1H have been omitted for clarity. Symmetry operation used to generate equivalent atoms ('): $1-x, 1-y, z$.

Received: October 2, 2014
Published online: December 21, 2014

Keywords: bioinorganic chemistry · copper · EPR spectroscopy · magnetic properties · peroxo complexes

[1] a) E. I. Solomon, J. W. Ginsbach, D. E. Heppner, M. T. Kieber-Emmons, C. H. Kjaergaard, P. J. Smeets, L. Tian, J. S. Woertink, *Faraday Discuss.* **2011**, *148*, 11 – 39; b) M. Rolff, J. Schottenheim, H. Decker, F. Tuczek, *Chem. Soc. Rev.* **2011**, *40*, 4077 – 4098.

[2] R. Balasubramanian, S. M. Smith, S. Rawat, L. A. Yatsunyk, T. L. Stemmler, A. C. Rosenzweig, *Nature* **2010**, *465*, 115 – 119.

[3] H. Decker, R. Dillinger, F. Tuczek, *Angew. Chem. Int. Ed.* **2000**, *39*, 1591 – 1595; *Angew. Chem.* **2000**, *112*, 1656 – 1660.

[4] a) W. B. Tolman, *Acc. Chem. Res.* **1997**, *30*, 227 – 237; b) P. L. Holland, W. B. Tolman, *Coord. Chem. Rev.* **1999**, *190 – 192*, 855 – 869.

[5] N. Kitajima, Y. Moro-oka, *Chem. Rev.* **1994**, *94*, 737 – 757.

[6] S. Itoh, S. Fukuzumi, *Acc. Chem. Res.* **2007**, *40*, 592 – 600.

[7] R. R. Jacobson, Z. Tyeklar, A. Farooq, K. D. Karlin, S. Liu, J. Zubieta, *J. Am. Chem. Soc.* **1988**, *110*, 3690 – 3692.

[8] N. Kitajima, K. Fujisawa, Y. Moro-oka, K. Toriumi, *J. Am. Chem. Soc.* **1989**, *111*, 8975 – 8976.

[9] J. A. Halfen, S. Mahapatra, E. C. Wilkinson, S. Kaderli, V. G. Young, L. Que, A. D. Zuberbühler, W. B. Tolman, *Science* **1996**, *271*, 1397 – 1400.

[10] L. M. Mirica, X. Ottenwaelder, T. D. P. Stack, *Chem. Rev.* **2004**, *104*, 1013 – 1045.

[11] a) C. Würtele, O. Sander, V. Lutz, T. Waitz, F. Tuczek, S. Schindler, *J. Am. Chem. Soc.* **2009**, *131*, 7544 – 7545; b) T. Hoppe, S. Schaub, J. Becker, C. Würtele, S. Schindler, *Angew. Chem. Int. Ed.* **2013**, *52*, 870 – 873; *Angew. Chem.* **2013**, *125*, 904 – 907.

[12] K. Komiyama, H. Furutachi, S. Nagatomo, A. Hashimoto, H. Hayashi, S. Fujinami, M. Suzuki, T. Kitagawa, *Bull. Chem. Soc. Jpn.* **2004**, *77*, 59 – 72.

[13] K. E. Dalle, T. Gruene, S. Dechert, S. Demeshko, F. Meyer, *J. Am. Chem. Soc.* **2014**, *136*, 7428 – 7434.

[14] a) M. Metz, E. I. Solomon, *J. Am. Chem. Soc.* **2001**, *123*, 4938 – 4950; b) E. I. Solomon, P. Chen, M. Metz, S.-K. Lee, A. E. Palmer, *Angew. Chem. Int. Ed.* **2001**, *40*, 4570 – 4590; *Angew. Chem.* **2001**, *113*, 4702 – 4724.

[15] a) F. Meyer, K. Heinze, B. Nuber, L. Zsolnai, *Chem. Soc. Dalton Trans.* **1998**, 207 – 213; b) J. Ackermann, F. Meyer, E. Kaifer, H. Pritzkow, *Chem. Eur. J.* **2002**, *8*, 247 – 258; c) J. Klingele, S. Dechert, F. Meyer, *Coord. Chem. Rev.* **2009**, *253*, 2698 – 2741.

[16] S. Buchler, F. Meyer, E. Kaifer, H. Pritzkow, *Inorg. Chim. Acta* **2002**, *337*, 371 – 386.

[17] A. Gondoh, T. Koike, M. Akita, *Inorg. Chim. Acta* **2011**, *374*, 489 – 498.

[18] M. Veronelli, N. Kindermann, S. Dechert, S. Meyer, F. Meyer, *Inorg. Chem.* **2014**, *53*, 2333 – 2341.

[19] A. Brinkmeier, Masters Thesis, Georg-August-Universität Göttingen, **2014**.

[20] Y. Lee, G. Y. Park, H. R. Lucas, P. L. Vajda, K. Kamaraj, M. A. Vance, A. E. Milligan, J. S. Woertink, M. A. Siegler, A. A. N. Sarjeant, L. N. Zakharov, A. L. Rheingold, E. I. Solomon, K. D. Karlin, *Inorg. Chem.* **2009**, *48*, 11297 – 12309.

[21] M. J. Henson, M. Vance, C. X. Zhang, H.-C. Liang, K. D. Karlin, E. I. Solomon, *J. Am. Chem. Soc.* **2003**, *125*, 5186 – 5192.

[22] a) U. Thewalt, G. Struckmeier, *Z. Anorg. Allg. Chem.* **1976**, *419*, 163 – 170; b) H. Mäcke, M. Zehnder, U. Thewalt, S. Fallab, *Helv. Chim. Acta* **1979**, *62*, 1804 – 18015; c) D. D. Dexter, C. N. Sutherby, M. W. Grieb, R. C. Beaumont, *Inorg. Chim. Acta* **1984**, *86*, 19 – 31.

[23] E. I. Solomon, F. Tuczek, D. E. Root, C. A. Brown, *Chem. Rev.* **1994**, *94*, 827 – 856.

[24] The Cu···Cu distance in **2** is also significantly shorter than in the pyrazolate-bridged subunits of a tetracopper(II) peroxo complex with fewer short-ligand chelate arms (3.902 Å): F. Meyer, H. Pritzkow, *Angew. Chem. Int. Ed.* **2000**, *39*, 2112 – 2115; *Angew. Chem.* **2000**, *112*, 2199 – 2202.

[25] A. W. Addison, T. N. Rao, J. Reedijk, J. van Rijn, G. C. Verschoor, *J. Chem. Soc. Dalton Trans.* **1984**, 1349 – 1356.

[26] K. W. H. Stevens, *Proc. R. Soc. London Ser. A* **1952**, *214*, 237 – 246.

[27] N. D. Chasteen, R. L. Belford, *Inorg. Chem.* **1970**, *9*, 169 – 175.

[28] I. Dzyaloshinsky, *J. Phys. Chem. Solids* **1958**, *4*, 241 – 255.

[29] T. Moriya, *Phys. Rev.* **1960**, *120*, 91 – 98.

[30] B. S. Tsukerblat, A. Tarantul, A. Müller, *J. Mol. Struct.* **2007**, *838*, 124 – 132.

[31] A. Tarantul, B. Tsukerblat, A. Müller, *Inorg. Chem.* **2007**, *46*, 161 – 169.

[32] B. S. Tsukerblat, M. I. Belinski, F. E. Fainzil′berg, *Sov. Sci. Rev. Sect. B* **1987**, *9*, 337.

[33] A. Bencini, D. Gatteschi, *Mol. Phys.* **1982**, *47*, 161 – 169.

[34] J. Yoon, E. I. Solomon, *Coord. Chem. Rev.* **2007**, *251*, 379 – 400.

[35] R. Maurice, A. M. Pradipto, N. Guihéry, R. Broer, C. de Graaf, *J. Chem. Theory Comput.* **2010**, *6*, 3092 – 3101.

